

# Barkhausen Noise and Critical Scaling in the Demagnetization Curve

John H. Carpenter and Karin A. Dahmen

University of Illinois at Urbana-Champaign, Department of Physics, 1110 West Green Street, Urbana, IL 61801.

(Dated: October 31, 2018)

The demagnetization curve, or initial magnetization curve, is studied by examining the embedded Barkhausen noise using the non-equilibrium, zero temperature random-field Ising model. The demagnetization curve is found to reflect the critical point seen as the system's disorder is changed. Critical scaling is found for avalanche sizes and the size and number of spanning avalanches. The critical exponents are derived from those related to the saturation loop and subloops. Finally, the behavior in the presence of long range demagnetizing fields is discussed. Results are presented for simulations of up to one million spins.

PACS numbers: 75.60.Ej, 64.60.Ht, 75.60.Ch

During the last decade, much progress has been made in the study of universality in hysteresis and avalanche type noise in both experiments and theory. Hysteresis in ferromagnets and associated Barkhausen noise have been studied in great detail as a conveniently accessible example system. The zero temperature non-equilibrium random field Ising model (RFIM) and recent variants have proven very successful in predicting universal scaling behavior in such systems [1, 2, 3]. In particular, an underlying disorder induced non-equilibrium phase transition has been found, which may be the cause of the broad range of power law scaling observed in many systems with avalanche-type noise. It is expected to be relevant to Barkhausen noise in disordered (hard) magnets [4]. For soft magnets, where the long range demagnetizing fields are important, the system appears to naturally operate at the single domain wall depinning point [3, 5, 6], thus being self organized critical [7].

So far, most of the theoretical studies of this scaling behavior have focused on the properties of the saturation hysteresis loop (except for some recent studies [8, 9, 10, 11, 12]). In this letter we report history induced scaling behavior for subloops and in particular the demagnetization curve. Ferromagnetic materials with a remnant magnetization can be demagnetized by applying an oscillating magnetic field with amplitude slowly decreasing from a large initial value to zero. Sometimes the final state is also termed AC-demagnetized state. The oscillating external field with decreasing amplitude takes the system through concentric subloops (Fig. 1). The line connecting the tips of the subloops is known as the *normal or initial magnetization curve*, or *demagnetization curve*. It is to be distinguished from the *virgin curve* which is obtained by thermal demagnetization [13]. We used the RFIM to simulate the demagnetization curve for different amounts of disorder, especially near the critical disorder mentioned above. It turns out that this curve reflects much of the scaling behavior found for the saturation hysteresis loop. This may be surprising, since the meta-stable states encountered in the demagnetization curve are completely different from those of the saturation

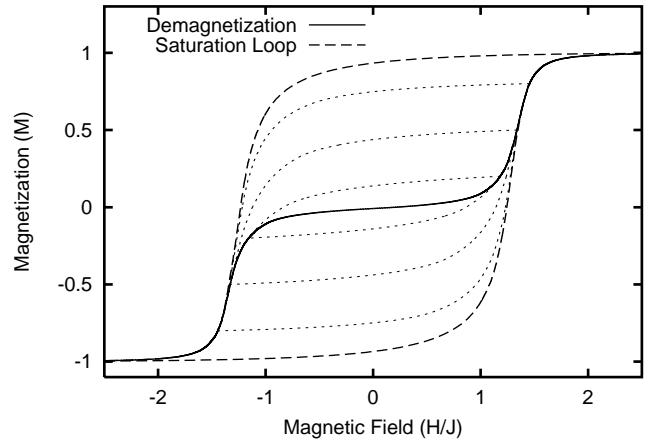


FIG. 1: The saturation hysteresis loop (dashed line) with its corresponding demagnetization curve (solid line) at a disorder of  $R = 2.9J$  in a  $100^3$  system. A few of the many subloops performed are shown as dotted lines.

tion loop. In the following we briefly describe the model, then derive the necessary exponent relations, discuss the numerical results, and their relevance to experiments.

In the RFIM the magnetic domains of a real magnet are modeled by spins  $s_i = \pm 1$  arranged on a hypercubic lattice. Nearest neighbors interact ferromagnetically through a positive exchange interaction  $J$ . Variants of the model for soft magnets include additional long-range interactions due to the demagnetizing field and the dipole-dipole interactions. All spins are coupled to a homogeneous external magnetic field  $H(t)$  that is varied adiabatically slowly. To model disorder in the system, a quenched random magnetic field  $h_i$  is added at each site, that is taken from a Gaussian probability distribution  $P(h_i) = \exp(-h_i^2/2R^2)/\sqrt{2\pi R}$ , whose width  $R$  is a measure of the amount of disorder in the system. We write the effective Hamiltonian for a system with  $N$  spins [2]:

$$\mathcal{H} = -J \sum_{\langle ij \rangle} s_i s_j - \sum_i (H(t) + h_i - J_{inf} M) s_i, \quad (1)$$

where  $J_{inf}$  is an infinite range demagnetizing field,  $M =$

$\sum_i s_i/N$  is the magnetization of the system, and  $\langle ij \rangle$  stands for nearest neighbor pairs of spins. Initially (at time  $t = -\infty$ ),  $H(-\infty) = -\infty$  and all the spins are pointing down. Each spin is always aligned with its local effective field  $h_i^{eff} = J \sum_{\langle ij \rangle} s_j + H(t) + h_i - J_{inf} M$ . The external field  $H(t)$  is slowly increased from  $-\infty$  until the local field,  $h_i^{eff}$ , of any spin  $s_i$  changes sign, causing the spin to flip [4]. Each spin flip can trigger coupled spins to flip as well, thus leading to an avalanche of spin flips. During such an avalanche the external magnetic field is kept fixed (adiabatic case). It is only changed in between successive avalanches, to trigger the next spin flip that seeds a new avalanche. The simulations are based on code both available on the web [14] and that obtained via correspondence [15] which has been modified to allow for subloops in the history. In the following we set  $J_{inf} = 0$ .

A similar process to the AC demagnetization of the laboratory is used in simulating the demagnetization curve. For a particular realization of random fields, the system is started at saturation (all spins aligned) and the field is then oscillated back and forth while being slowly reduced in magnitude. For an exact demagnetization, the field reversal points are sufficiently reduced so that the last avalanche of spins does not align with the field. One may also perform a non-exact demagnetization by reducing the field by a fixed amount  $\Delta H$  each oscillation.

Such a field history produces an infinite set of nested subloops. The demagnetization curve itself is then composed of the last avalanche of each subloop, which brings the field back to its return point. By examining the scaling behavior of these subloops one should then be able to determine the corresponding behavior for the demagnetization curve.

The scaling behavior of subloops has been shown to be dependent on that of the saturation loop plus one new exponent [8, 9]. The scaling forms for the saturation loop and subloops may be combined to give a general form dependent on the field  $H$ , disorder  $R$ , subloop return point magnetization  $M_{max}$ , and the parameter of interest. In particular, near the critical point the avalanche size distribution scales as

$$D(S, H, R, M_{max}) \sim S^{-\tau} \mathcal{D}(S^{\sigma\beta\delta} h', S^{\sigma} r, S^{\sigma'} \epsilon), \quad (2)$$

the correlation function as

$$G(x, H, R, M_{max}) \sim x^{-1/(d-2+\eta)} \mathcal{G}(x/\xi(r, h', \epsilon)) \quad (3)$$

where  $\xi(r, h', \epsilon) \sim r^{-\nu} \mathcal{Y}(h'/r^{\beta\delta}, r^{-\nu/\nu'} \epsilon)$ , and the number of spanning avalanches scales as

$$N(L, H, R, M_{max}) \sim L^{\theta+\beta\delta/\nu} \mathcal{N}(L^{1/\nu} r, L^{1/\nu'} \epsilon, h'/r^{\beta\delta}). \quad (4)$$

Here  $h' \equiv h + Br + B_h \epsilon$  is the tilted scaling axis, where  $B$  and  $B_h$  are non-universal constants, with  $h = H - H_c^d$ ,  $r = (R - R_c)/R$ , and  $\epsilon = (M_{max_c} - M_{max})/M_{max}$  [8, 9, 16, 17]. Note that as the last avalanche in a subloop

occurs at  $M_{max}$ ,  $M_{max}$  also lies on the demagnetization curve so that  $M_{max_c} = M_c^d$ . The critical point of the demagnetization curve is at  $(H_c^d, M_c^d)$ . Corrections to  $r$  and  $\epsilon$  are not significant for the following calculations.

For  $\epsilon > 0$  subloops are steepest at their endpoints, where  $h' = 0$ . From this one may construct the scaling forms for the demagnetization curve by realizing that at  $h' = 0$  the forms for subloops and the demagnetization curve must be identical. As an example, the avalanche size distribution would give  $D_d(S, H, R) = D(S, H, R, M_{max})$  at  $h' = 0$  or equivalently  $S^{-\tau_d} \mathcal{D}_d(S^{\sigma_d \beta_d \delta_d} h'_d, S^{\sigma_d} r) = S^{-\tau} \mathcal{D}(0, S^{\sigma} r, S^{\sigma'} \epsilon)$  where subscript  $d$  denotes quantities associated with the demagnetization curve and  $h'_d = h + B_d r$ . Notice that  $h' = 0$  implies  $\epsilon = -(h + Br)/B_h$  so that both sides have the same functional dependence. From this we may read off that one expects  $\tau_d = \tau$ ,  $B_d = B$ ,  $\sigma_d \beta_d \delta_d = \sigma'$ , and  $\sigma_d = \sigma$ .

The integrated avalanche size distribution for the demagnetization curve is obtained by integrating over the field  $h'_d$  which is equivalent to integrating over  $\epsilon$  at  $h' = 0$ . Performing this integration yields

$$D_d^{int}(S, R) \sim S^{-(\tau_d + \sigma_d \beta_d \delta_d)} \mathcal{D}_d^{int}(S^{\sigma_d} r) \sim S^{-(\tau + \sigma')} \mathcal{D}^{int}(S^{\sigma} r). \quad (5)$$

From this one obtains another scaling relation,  $\tau_d + \sigma_d \beta_d \delta_d = \tau + \sigma'$ .

A similar analysis of the correlation function yields the relations  $\nu_d = \nu$ ,  $\beta_d/\nu_d = (\beta - \beta\delta + \sigma'/\sigma)/\nu$ , and  $\eta_d = \eta$ . Also, integrating the number of spanning avalanches over  $\epsilon$  yields the additional relation  $\theta_d = \theta + (\beta\delta - \sigma'/\sigma)/\nu$ . The associated scaling forms are

$$G_d^{int}(x, R) \sim x^{-(d+\beta_d/\nu_d)} \mathcal{G}_d^{int}(x r^{\nu_d}) \quad (6)$$

and

$$N_d^{int}(L, R) \sim L^{\theta_d} \mathcal{N}_d^{int}(L^{1/\nu_d} r) \quad (7)$$

respectively. It is possible to determine other relations, but from these we have already determined all the demagnetization exponents from those associated with the saturation loop and subloops. A summary of these relations is given in Table I. Note that all demagnetization quantities may be expressed as the corresponding saturation loop value plus a function of the saturation loop exponents times a correction factor  $X' \equiv (\beta\delta - \sigma'/\sigma)/\nu = \beta\delta/\nu - \beta_d \delta_d/\nu_d$  (see Table I).

The integrated avalanche size distribution was measured on the demagnetization curve in systems with  $100^3$  spins for several disorders above the critical disorder. The resulting distributions are shown in Figure 2. As with the saturation loop, the cutoff size is found to increase as the disorder approaches the critical disorder. The avalanche distributions were collapsed using the scaling ansatz given by Eq. 5 and are shown in the inset of Fig. 2. Within errorbars, the resulting scaling function

TABLE I: Relations between exponents describing the saturation loop (unprimed), subloops (primed), and demagnetization curve (subscript  $d$ ) scaling behaviors.

Relation	Source
$\tau_d + \sigma_d \beta_d \delta_d = \tau + \sigma \beta \delta - \sigma \nu X'$	$D_{int}(S, R)$
$\beta_d / \nu_d = \beta / \nu - X'$	$G_{int}(x, R)$
$\sigma_d = \sigma$	$D_{int}(S, R)$
$\theta_d = \theta + X'$	$N(L, R)$
$\tau_d = \tau$	$D(S, R, H)$
$\nu_d = \nu$	$G_{int}(x, R)$

$X' = (\beta \delta - \sigma' / \sigma) / \nu = {}^a (\beta \delta - \beta_d \delta_d) / \nu$

<sup>a</sup>From relations 1, 3, and 5.

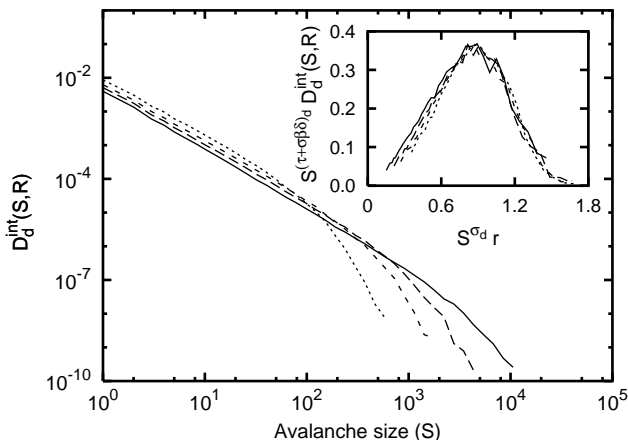


FIG. 2: Integrated avalanche size distribution curves for  $100^3$  systems at disorders  $R = 2.5J, 2.7J, 2.9J,$  and  $3.3J$  and averaged over 10, 5, 4, and 1 random seeds respectively. The scaling collapse is shown in the inset where  $r = (R - R_c) / R$  with  $R_c = 2.12J$ . The critical exponents are  $(\tau + \sigma \beta \delta)_d = 2.1$  and  $1 / \sigma_d = 4.1$ .

is identical in form to that found for the saturation loop multiplied by a constant. The resulting exponents are listed in Table II and are consistent with the relations (Table I) predicted from the previous analysis. Spin-flip correlation functions also collapse according to Eq. 6 [9]. The measured exponents are listed in Table II.

Although  $\beta_d / \nu_d$  was measured in the correlation function collapse, due to its small magnitude the value cannot be reliably extracted from the dimension of the system in the equation  $d + \beta_d / \nu_d$ . However, one may directly measure  $\beta_d / \nu_d$  from  $\Delta M_d^{int}$ , the change in magnetization due to all system spanning avalanches [16]. For the demagnetization curve, the scaling form is

$$\Delta M_d^{int} \sim L^{-\beta_d / \nu_d} \Delta \mathcal{M}_d^{int}(L^{1/\nu_d} r). \quad (8)$$

The jump in magnetization was measured for system sizes of  $20^3, 40^3, 70^3,$  and  $100^3$  for a range of disorders. The resulting curves are shown in Fig. 3 with a scaling collapse

TABLE II: Universal critical exponents found from scaling collapses for both the demagnetization curve and saturation hysteresis loop.

Exponent	Demagnetization	Saturation <sup>a</sup>
$\tau + \sigma \beta \delta$	$2.10 \pm 0.05$	$2.03 \pm 0.03$
$1 / \sigma$	$3.9 \pm 0.4$	$4.2 \pm 0.3$
$d + \beta / \nu$	$3.1 \pm 0.2$	$3.07 \pm 0.30$
$1 / \nu$	$0.71 \pm 0.10$	$0.71 \pm 0.09$
$\theta$	$0.01 \pm 0.01$	$0.015 \pm 0.015$
$\beta / \nu$	$0.03 \pm 0.02$	$0.025 \pm 0.020$

<sup>a</sup>Reference [16, 17]

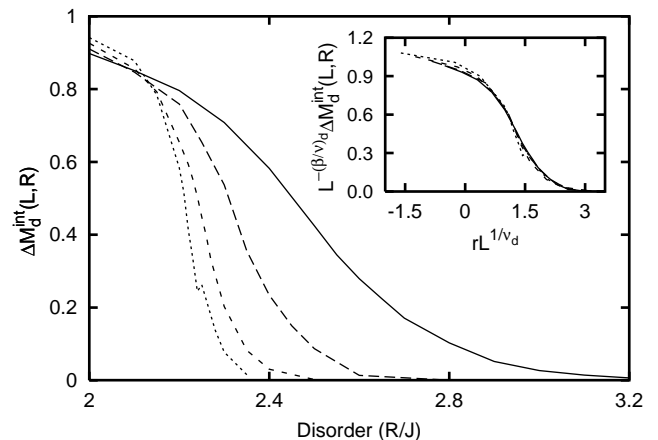


FIG. 3: Size of the magnetic discontinuity  $\Delta M_d^{int}$  due to system spanning avalanches for system sizes of  $20^3, 40^3, 70^3,$  and  $100^3$  averaged over 400, 60, 80, and 10 random configurations respectively. Curves are collapsed using  $r = (R - R_c) / R$  with  $R_c = 2.12J$ . The inset shows the collapse using the critical exponents  $\beta / \nu = 0.03$  and  $1 / \nu = 0.71$ .

using Eq. 8 in the corresponding inset. The exponents are listed in Table II.

The number of system spanning avalanches in the demagnetization curve was also measured for the same systems as used in the size of spanning avalanches collapse. The resulting exponents are listed in Table II. Due to fluctuations the curves do not collapse well near their peak values. The exponent  $\theta_d$ , which scales the peak value, has thus been left with a large uncertainty and could possibly vanish [9].

Comparing the exponents from the two finite size scaling collapses shows that the values of  $1 / \nu$  are in excellent agreement with the prediction that they should be equal in the saturation loop and demagnetization curve. Similarly, the two exponents governing the power-law behavior at the critical point are found to differ from the saturation loop values, as predicted. However the error bars have significant overlap. A simpler relation may be obtained by adding the equations for  $\theta_d$  and  $\beta_d / \nu_d$  giving

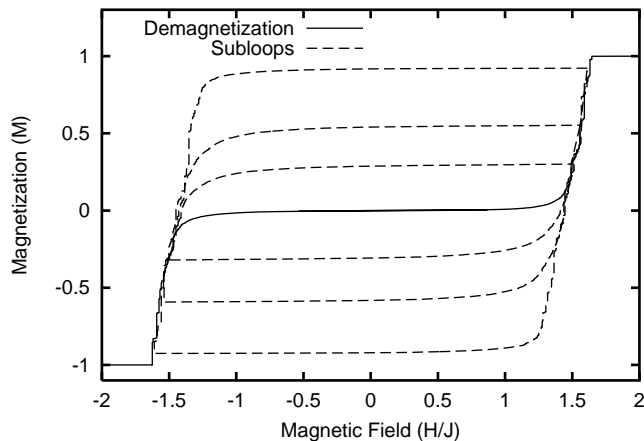


FIG. 4: The demagnetization curve (solid line) and several subloops (dashed lines) at a disorder of  $R = 1.8J$  and  $J_{inf} = 0.25J$  in a  $100^3$  system.

$\theta_d + \beta_d/\nu_d = \theta + \beta/\nu$  which is satisfied by the measured exponents. The value of the correction factor may be estimated from the finite size scaling exponents giving  $X' = -0.005 \pm 0.005$ . The power law exponent from the avalanche size distribution also contains the correction factor, but due to relatively small system sizes, finite size effects do not allow one to reliably extract  $X'$ . While  $X'$  was found to be slightly negative, because of the large uncertainty in the critical exponents for both the saturation loop and demagnetization curve, one cannot rule out the possibility that  $X'$  vanishes (as occurs on the Bethe lattice [20]). If such were the case then all the critical exponents would be identical for both the saturation loop and demagnetization curve.

In the above analysis we have ignored long-range demagnetizing fields. To examine the effect of such fields one now sets  $J_{inf} > 0$  in the Hamiltonian, Eq. 1. A demagnetization process may again be applied to the system by applying an oscillating field and decreasing it by a given  $\Delta H$  each oscillation. The resulting curves for a  $100^3$  system at a disorder of  $R = 1.8J$  with  $J_{inf} = 0.25J$  are shown in Fig. 4. For clarity only a few subloops are shown. All the curves, including the demagnetization curve, show a linear  $M(H)$  behavior as the field is increased, as one would expect for a system undergoing domain wall propagation. Additionally, for the same curves one finds a power law distribution of avalanche sizes, as expected for a self organized critical system [5, 6]. Preliminary experimental results by A. Mills and M. B. Weissman using a soft magnetic material suggest the results of Fig. 4 are correct [18].

In the absence of long range demagnetizing fields, the demagnetization curve of the RFIM exhibits disorder induced critical scaling in quantities associated with its Barkhausen noise. Additionally there are no new independent critical exponents, rather all may be derived

from those of the saturation loop and subloops. Experiments to confirm such behavior have not yet been performed, but hard magnets or systems where disorder dominates are expected to exhibit such behavior [19]. Soft magnets are not expected to exhibit such behavior as realized when long range demagnetizing fields are included in the RFIM. The system is then self organized critical, with power law distributions of avalanches for both the saturation loop and subloops.

We thank Jim Sethna, Andy Mills, and Mike Weissman, for very useful discussions. This work was supported by NSF grants DMR 99-76550 and DMR 00-72783. K. D. also gratefully acknowledges support from an A. P. Sloan fellowship. We also thank IBM for a generous equipment award and the Materials Computation Center for the use of their IBM Workstation Cluster.

- 
- [1] K. Dahmen and J. P. Sethna, Phys. Rev. B **53**, 14872 (1996).
  - [2] M. C. Kuntz and J. P. Sethna, Phys. Rev. B **62**, 11699 (2000).
  - [3] J. P. Sethna, K. A. Dahmen, and C. R. Myers, Nature **410**, 242 (2001).
  - [4] J. P. Sethna, K. Dahmen, S. Kartha, J. A. Krumhansl, B. W. Roberts, and J. D. Shore, Phys. Rev. Lett. **70**, 3347 (1993).
  - [5] P. Cizeau, S. Zapperi, G. Durin, and H. E. Stanley, Phys. Rev. Lett. **79**, 4669 (1997).
  - [6] S. Zapperi, P. Cizeau, G. Durin, and H. E. Stanley, Phys. Rev. B **58**, 6353 (1998).
  - [7] P. Bak, C. Tang, and K. Wiesenfeld, Phys. Rev. A **38**, 364 (1988).
  - [8] J. H. Carpenter, K. A. Dahmen, J. P. Sethna, G. Friedman, S. Loverde, and A. Vanderveld, J. Appl. Phys. **89**, 6799 (2001).
  - [9] J. H. Carpenter and K. A. Dahmen, in preparation.
  - [10] L. Dante, G. Durin, A. Magni, and S. Zapperi, cond-mat/0106331.
  - [11] S. Zapperi, A. Magni, and G. Durin, cond-mat/0106332.
  - [12] F. Colaiori, A. Gabrielli, and S. Zapperi, cond-mat/0112190.
  - [13] G. Bertotti, *Hysteresis in Magnetism* (Academic Press, 1998).
  - [14] For a fun and instructive numerical simulation written by Matthew C. Kuntz and J. P. Sethna (with source code) of the non-equilibrium zero temperature RFIM visit, URL <http://www.lassp.cornell.edu/sethna/hysteresis/code>.
  - [15] J. P. Sethna, private communication.
  - [16] O. Perković, K. A. Dahmen, and J. P. Sethna, Phys. Rev. B **59**, 6106 (1999).
  - [17] O. Perković, K. Dahmen, and J. P. Sethna, Phys. Rev. Lett. **75**, 4528 (1995).
  - [18] A. Mills and M. B. Weissman, private communication.
  - [19] A. Berger, A. Inomata, J. S. Jiang, J. E. Pearson, and S. D. Bader, Phys. Rev. Lett. **85**, 4176 (2000).
  - [20] Reference [12] finds  $\beta_d = \beta$  for the RFIM on the Bethe lattice. The exponent relations of Table I give  $X' = 0$ .